STRUCTURE FUNCTION AND QCD RESULTS FROM THE CCFR NEUTRINO EXPERIMENT AT THE FERMILAB TEVATRON

M.H.Shaevitz, C.G.Arroyo, K.T.Bachmann, A.O.Bazarko, R.E.Blair,
T.Bolton, C.Foudas, B.J.King, W.C.Lefmann, W.C.Leung, W.G. Seligman,
S.R.Mishra, E.Oltman, P.Z.Quintas, S.A.Rabinowitz, F.J.Sciulli
Nevis Labs, Columbia University, Irvington, NY 10533

F.S.Merritt, M.J.Oreglia, B.A. Schumm
University of Chicago, Chicago IL 60637

R.H.Bernstein, F.Borcherding, H.E.Fisk, D.D.Yovanovitch,
M.J.Lamm, W.Marsh, K.W.B.Merritt, H.Schellman
Fermilab, Batavia, IL 60510

A.Bodek, H.S.Budd, P.DeBarbaro, W.K.Sakumoto
University of Rochester, Rochester, NY 14627

T.Kinnel, P.H.Sandler, W.H.Smith
University of Wisconsin, Madison, WI 53706

Talk Presented by M.H. Shaevitz at the
Recontres De Physique De La Vallee D'Aoste
March, 1992

Abstract

We present measurements of the nucleon structure functions $F_2(x,Q^2)$ / $xF_3(x,Q^2)$ and the strange quark distribution function $s(x,Q^2)$ derived from ν_μ ($\bar{\nu}_\mu$)-Fe charged-current interactions. The results were taken from a sample of 1,280,000 ν_μ and 270,000 $\bar{\nu}_\mu$ events obtained in two runs of the Fermilab Tevatron quad-triplet beam using the Lab E neutrino detector. The non-singlet (xF_3) evolution is found to be consistent with $\Lambda_{\overline{MS}} = 210 \pm 28(stat.) \pm 41(syst.)$ MeV. The simultaneous singlet and non-singlet analysis of F_2 and xF_3 yields a value of $\Lambda_{\overline{MS}} = 225 \pm 50$ MeV, with a gluon distribution given by $xG(x,Q^2 = 5\text{GeV}^2) \propto (1-x)^{\eta_g}$ with $\eta_g = 4.4 \pm 1.9$. The strange quark distribution is found from a next-to-leading-order analysis of $\nu_\mu(\bar{\nu}_\mu)$ charm production identified as dimuon events in the above charged-current sample. The analysis yields a value of $m_c = 1.61 \pm 0.26$ GeV and $\kappa = \frac{2S}{U+D} = .435 \pm .059$. Comparisons of our F_2 structure function results with charged-lepton scattering indicate good agreement above $x = .1$ but a 5 to 10 % discrepency below that value. Recent global fits by the CTEQ collaboration that explain this discrepancy as a growth of the strange sea at low x are shown to be inconsistent with our dimuon measurements.

1. Introduction

Neutrino scattering measurements provide a unique method for measuring both the $F_2(x,Q^2)$ and $xF_3(x,Q^2)$ structure functions which are associated, in the quark parton model, with the total quark ($q+\bar{q}$) and valence quark ($q-\bar{q}$) momentum distributions, respectively. The predicted Q^2 evolution of xF_3 is particularly simple since it is not coupled to the unknown gluon distribution and, therefore, can be used as a unambiguous test of perturbative Quantum Chromodynamics and measurement of $\Lambda_{\overline{MS}}$. Combined analyses of F_2 and xF_3 allow the separation of the gluon evolution

component and lead to information on the gluon structure function. In addition, neutrino charm production, which can be extracted from the observed dimuon events, allows the strange-quark sea to be investigated.

The differential cross-section for charged current interactions is given by:

$$\frac{d^2\sigma^{\nu(\overline{\nu})}}{dxdy} = \frac{G^2 s}{2\pi}\left[\left(1-y-\frac{Mxy}{2E}\right)F_2(x,Q^2)+\frac{y^2}{2}2xF_1(x,Q^2)\pm y(1-\frac{y}{2})xF_3(x,Q^2)\right] \quad (1)$$

We extract the structure functions from the measured number of $\nu_\mu(\overline{\nu}_\mu)$ events and the incident neutrino flux. The results reported here are from data taken in two runs using the Fermilab Tevatron quad-triplet beam with neutrino energies up to 600 GeV. A sample of 3,700,000 triggers was reduced after fiducial and kinematic cuts ($P_\mu > 15$ GeV, $\theta_\mu < .150$, and $E_{HAD} > 10$ GeV) to 1,280,000 ν_μ and 270,000 $\overline{\nu}_\mu$ induced events.

2. Detector Calibration and Flux Determination

The CCFR Lab E neutrino detector consists of a target calorimeter with iron plates, scintillation counters, and drift chambers followed by a solid iron toroid muon spectrometer. The detector was calibrated using charged particle test beams directed into the apparatus. For the hadron energy calibration,[1] a hadron beam was directed into the target at various energies and positions. Each beam particle was momentum analyzed to better than one percent leading to a resolution function known over three decades and an absolute calibration known to $\approx$ 1%. Test beam muons were used to calibrate the toroid spectrometer[2] giving an absolute calibration known to $\sim$ .6%. The muon resolution function is dominated by multiple scatttering and energy loss mechanisms in the iron toroid, which were simulated using Monte Carlo techniques and found to agree with the test beam results over three decades. Measurements of the structure function scaling violations are most sensitive to the relative calibration of the muon and hadron energies; a 1% relative change can induce a 50 MeV error in $\Lambda_{\overline{MS}}$. This relative calibration has been determined by forcing E_{VIS} (= E_{HAD}+ P_μ) to be independent of $y = E_{HAD}/E_{VIS}$ after Monte Carlo corrections for acceptance. The necessary corrections to $P_\mu(E_{HAD})$ are .995(1.017), consistent with the test beam absolute calibrations.

The neutrino flux determination is broken into two parts. First, the absolute flux is found from the observed events and the world average measured total cross-section, $\sigma^{\nu N} = 0.676\pm0.014\times 10^{-38} cm^2 E_\nu(GeV)$. Next, the relative flux at different energies for both ν_μ and $\overline{\nu}_\mu$'s is determined from the subset of events with low hadron energy, $E_{HAD} < 20$ GeV. (The cross-section for these events has been shown,[3] up to small corrections, to be independent of energy and the same for both ν_μ and $\overline{\nu}_\mu$ interactions) This technique is statistically limited and introduces an error of less than 1% for the relative flux determination.

3. Structure Function Extraction

For the structure function extraction, additional cuts were imposed ($Q^2 > 1$ GeV^2 and $E_\nu > 50$ GeV) and the data were separated into twelve x bins from .015 to .850 and sixteen Q^2 bins from 1 to 600 GeV^2. Integrating the differential cross-section (See Eq. 1.) times flux over each (x, Q^2) bin yields two equations for the number of $\nu_\mu(\overline{\nu}_\mu)$ events in terms of the two structure functions F_2 and xF_3. The observed numbers of events are corrected by Monte Carlo techniques for acceptance and resolution smearing. To solve the two equations, we assume a parameterization of R determined from SLAC measurements[4] and apply isoscaler corrections for the 6.85% excess of neutrons over protons in iron. Based on our measurements[5] of dimuon production, we include scattering off strange sea quarks and a slow-rescaling threshold suppression for the production of charm quarks. Radiative corrections[6] are applied, and the cross-section is corrected for the massive W-boson propagator. The F_2 and xF_3 structure functions[7] extracted with this procedure are shown in Figure 1 along with the next-to-leading fits described in the next section.

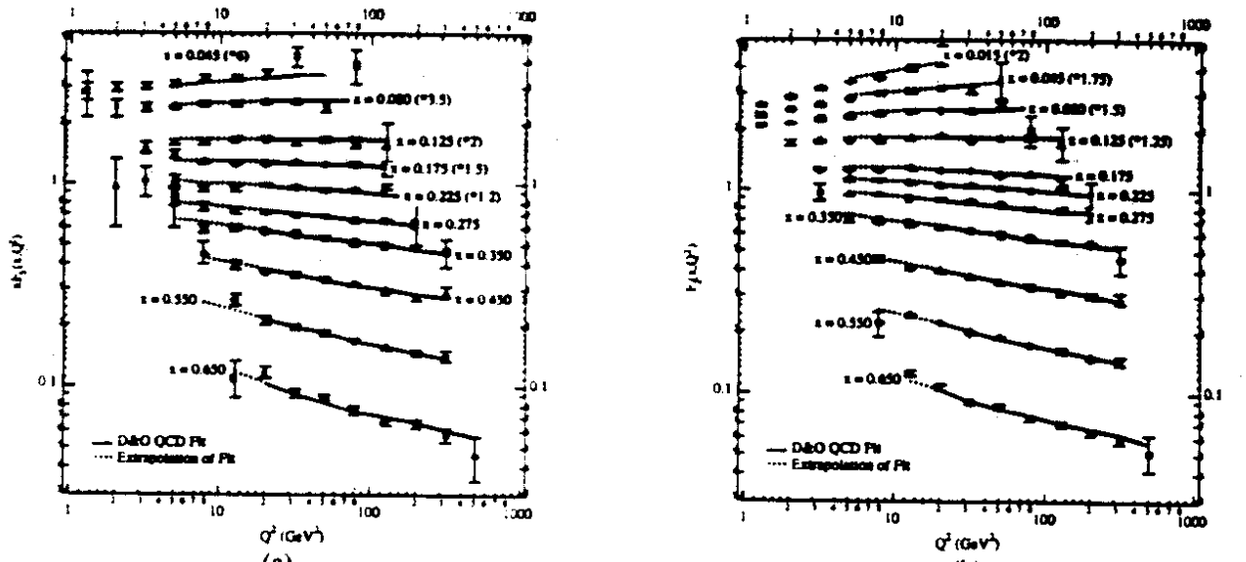

Figure 1: CCFR neutrino-iron structure functions a) xF_3 and b) F_2. The solid line is the NLO QCD prediction obtained from the combined xF_3 / F_2 fit. The dotted line is an extrapolation of the QCD fit to regions outside the kinematic cuts for the fit.

4. $xF_3(x,Q^2)$ and $F_2(x,Q^2)$ Results

The xF_3 or valence structure function is predicted to have a simple QCD evolution independent of R and gluons. To leading order, the xF_3 evolution is given by:

$$\frac{dxF_3(x,Q^2)}{dlnQ^2} = \frac{\alpha_s(Q^2)}{\pi}\int_x^1 P_{qq}(z)\; xF_3(\frac{x}{z},Q^2)\;\frac{dz}{z} \tag{2}$$

As shown in Figure 1, the measured xF_3 evolution agrees well with the predicted QCD scaling violations obtained from a next-to-leading order (NLO) fit.[8] The fit includes target mass corrections and cuts of $Q^2 > 15$ GeV^2 to eliminate the non-perturbative region and $x < 0.7$ to remove the highest x bins where resolution corrections are sensitive to Fermi motion. The statistical precision of the fit can be improved by substituting F_2 for xF_3 at values of $x > .5$. The evolution of F_2 should conform to that of a non-singlet structure function in this high-x region where the effects of antiquarks, gluons, and the longitudinal structure function are negligible. This combined fit yields the value (for four quark flavors):

$$\Lambda^{(4)}_{\overline{MS}} = 210 \pm 28 \pm 41 \text{ MeV for } Q^2 > 15 \text{ GeV}^2 \tag{3}$$

where the first error is statistical and second error is systematic. The χ^2 for the fit is 60 for 52 degrees of freedom. This value of $\Lambda^{(4)}_{\overline{MS}}$ yields the following value for the strong coupling constant in next-to-leading order:

$$\alpha_s(Q^2 = M_Z^2) = .111 \pm .002 \pm .003 \tag{4}$$

The evolution of the F_2 structure function is dependent on the gluon distribution as indicated in the leading order expression:

$$\frac{dF_2(x,Q^2)}{dlnQ^2} = \frac{\alpha_s(Q^2)}{\pi}\left[\int_x^1 P_{qq}(z)\; F_2(\frac{x}{z},Q^2)\;\frac{dz}{z} + \int_x^1 P_{qG}(z)\; xG(\frac{x}{z},Q^2)\;\frac{dz}{z}\right] \tag{5}$$

This dependence allows the gluon distribution to be determined from a simultaneous fit to $F_2(x,Q^2)$ and $xF_3(x,Q^2)$. In this fit, the gluon distribution is parameterized by the functional

form $xG(x, Q_0^2 = 5GeV^2) = A_g(1-x)^{\eta_g}$ where A_g is fixed by the momentum sum rule. Using the NLO fitting program,[8] the simultaneous fit yields the values:

$$\Lambda^{(4)}_{\overline{MS}} = 225 \pm 30 \pm 40 \text{ MeV for } Q^2 > 15 \text{ GeV}^2 \quad (6)$$

and

$$\eta_g = 4.45 \, ^{+1.65}_{-1.15} \pm 1.25 \text{ at } Q_0^2 = 5GeV^2 \quad (7)$$

where in both cases the first error is statistical and the second is systematic. The χ^2 for the fit shown in Figure 1 is 118 for 106 degrees of freedom and the value of $\Lambda_{\overline{MS}}$ is consistent with the value from the non-singlet analysis indicating good agreement with the expected QCD phenomenology.

5. Neutrino Dimuon Production

The distinctive opposite sign dimuon signature serves as a unique and highly sensitive probe of the strange sea content of the nucleon through neutrino charm production.

$$\nu_\mu + \begin{pmatrix} s \\ d \end{pmatrix} \longrightarrow \mu^- + c \hookrightarrow s \, \mu^+ \, \nu_\mu$$

(The similar $\bar{\nu}_\mu$ process would have the s, d, and c quarks replaced by their antiquark partners and oppositely charged muons.) The strange quark distribution function is of particular theoretical interest in the exploration of higher order corrections, while the threshold behavior associated with the heavy charm mass is critical to the extraction of the weak mixing angle, $sin^2\theta_W$, from neutrino neutral current data. The heavy charm quark is expected to introduce an energy threshold in the dimuon production rate. This effect has been described in the past through the slow rescaling model, in which ξ, the momentum fraction carried by the struck quark, is related to the kinematic variable $x = Q^2/2M\nu$ by the expression $\xi = x(1+m_c^2/Q^2)$. Representing the momentum distribution of the s and d quarks within the nucleon as $\xi s(\xi)$ and $\xi d(\xi)$ and neglecting Callen-Gross violations, the leading-order cross section for neutrino production of dimuons is given by:

$$\frac{d^2\sigma(\nu N \rightarrow \mu^-\mu^+ X)}{d\xi \, dy} = \frac{G^2 2ME_\nu}{\pi} \left(\xi d(\xi)|V_{cd}|^2 + \xi s(\xi)|V_{cs}|^2\right) \left(1 - \frac{m_c^2}{2ME_\nu \xi}\right) D(z) \, B_c \quad (8)$$

where the function $D(z)$ describes the fragmentation of charm quarks into charmed hadrons and B_c is the semileptonic branching ratio for charmed hadrons. The analogous equation for antineutrinos is found by substituting $d(\xi) \rightarrow \bar{d}(\xi)$ and $s(\xi) \rightarrow \bar{s}(\xi)$.

With the kinematic cuts $P_{\mu_1} \geq 9$ GeV/c, $P_{\mu_2} \geq 5$ GeV/c, and $30 \leq E_\nu \leq 600$ GeV, a sample of 5030 ν_μ and 1060 $\bar{\nu}_\mu$ induced $\mu^\mp \, \mu^\pm$ events is observed with $\langle Q^2 \rangle = 22.2\text{GeV}^2/c^2$. Muonic decays of non-prompt π and K mesons comprise the primary dimuon background of 796.5 ± 11.5 ν_μ and 118.0 ± 2.1 $\bar{\nu}_\mu$ events to the above sample.[9] A leading-order analysis of these data has been reported previously.[5]

Recently, there has been much theoretical work[10] to extend the leading-order formalism of neutrino charm production to higher orders. Since a dominant contribution to this process is scattering off strange sea quarks, it is expected that the next-to-leading-order terms due to gluon quark-pair splitting will be significant. Further, a next-to-leading order analysis of the dimuon data should produce results for m_c that are comparable to similar analyses of charm photo- and lepto-production.

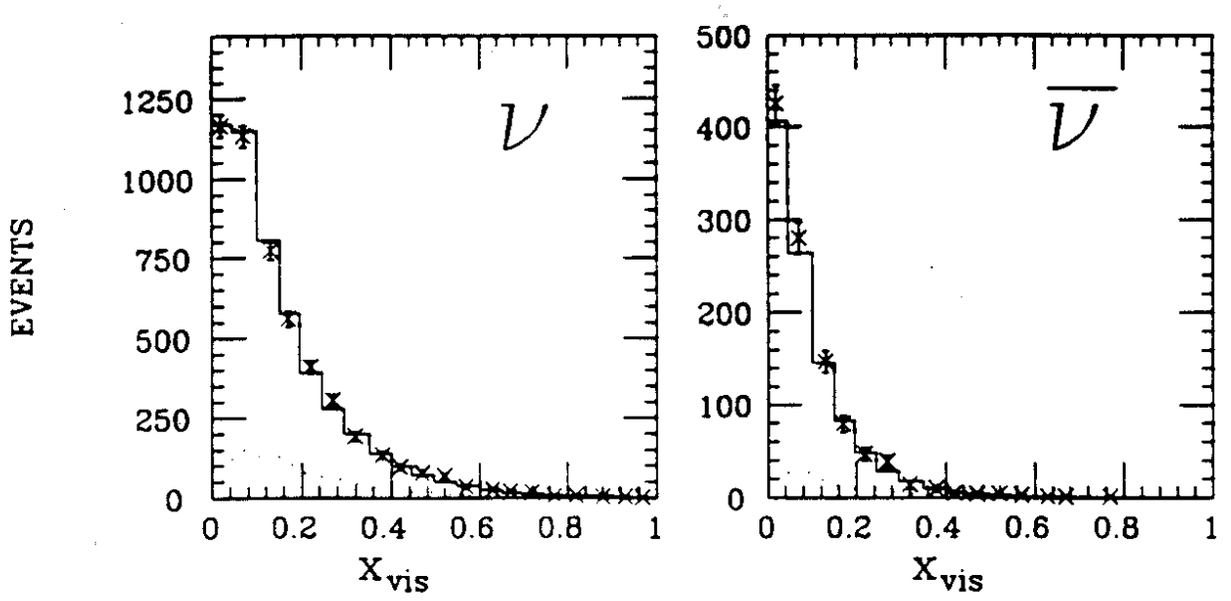

Figure 2: The x-distribution of the observed dimuon data for ν_μ (left) and $\bar{\nu}_\mu$ (right) induced events. Also shown are the predictions of the NLO fit (solid line) and the π/K background (dotted line).

We have used the Aivasis, Olness, and Tung next-to-leading order programs[10] in a fit to the dimuon data to extract the relevant physics parameters. The procedure involves comparing the number of data events in x and E_ν bins with a prediction from a Monte Carlo simulation. The simulation uses the quark and antiquark momentum densities obtained from the structure functions described in Section 4. The strange quark x dependence is assumed to be related to the $\bar{q}$ distribution by $xs(x) \propto (1-x)^\alpha\ x\bar{q}(x)$ with the magnitude set by the parameter $\kappa = 2S/(\overline{U}+\overline{D})$ where $S = \int_0^1 xs(x)\,dx$, etc. The overall normalization is set by the ratio of data to Monte Carlo for the charged-current single muon events. The results of the fit are shown in Figures 2 and 3. The extracted parameters are presented in the following table along with the previous leading-order results.[5]

	κ	α	m_c	B_c
NLO Fit	.435± .059	-0.27± .72	1.61± .26	.102± .009
LO Fit	.373± .048	2.50± .66	1.31± .24	.105± .008

6. Comparisons to Lepton Scattering

The F_2 structure function is accessible both through charged lepton and neutrino scattering. The lepton and neutrino structure functions are related to leading order by the "mean square charge" relationship:

$$\frac{F_2^{lN}}{F_2^{\nu N}} = \frac{5}{18}\left(1 - \frac{3}{5}\frac{s+\bar{s}}{q+\bar{q}}\right)$$

Our CCFR results span the Q^2 range from the low energy SLAC[11] (eD) region through the range covered by the NMC[12] and BCDMS[13] (μD) measurements as shown in Figure 4. For this comparison, the deuterium data has been corrected to iron using the F_2^{eFe}/F_2^{eD} ratio measured by SLAC[14] and NMC.[12] The results are in good agreement for $x > .1$ but show a

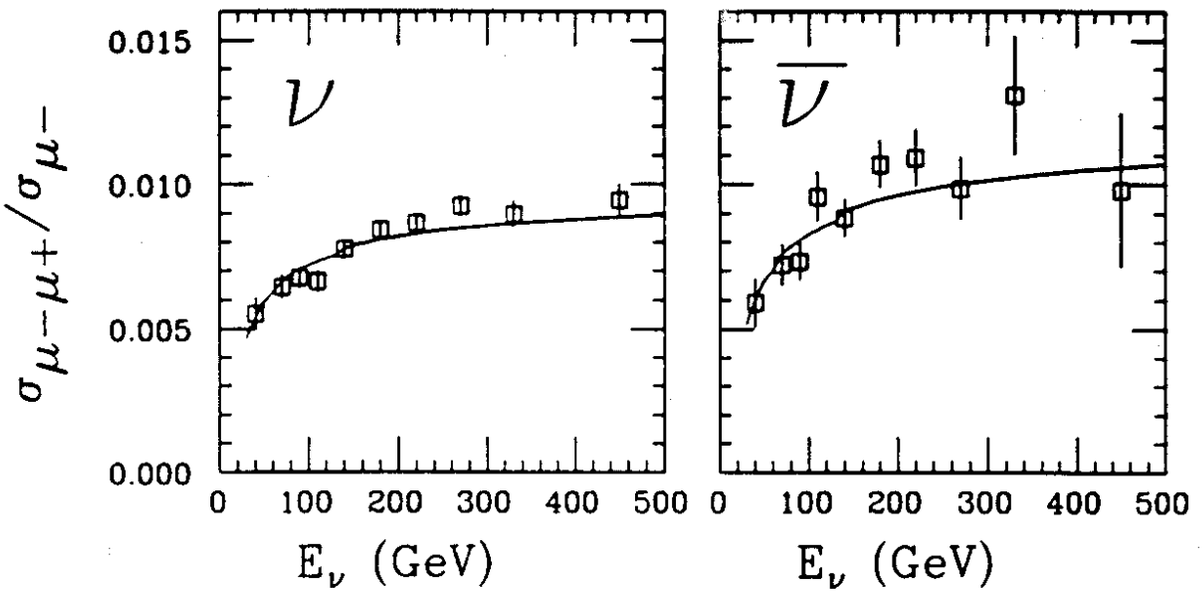

Figure 3: The dimuon rate versus E_ν for ν_μ (left) and $\bar{\nu}_\mu$ (right) data. The rates are corrected for acceptance, smearing, and kinematic cuts. Also shown are the predictions of the NLO fit (solid line) as described in the text.

5 to 10% discrepancy between the neutrino and muon results for lower x. The source of this small disagreement is at present not known. Possible sources include experimental systematic errors related to normalization and calibration or theoretical uncertainties associated with the heavy target correction and next-to-leading order effects. Recent global fits by the CTEQ[15] collaboration have attributed the muon versus neutrino difference to an enhanced strange sea at low x. This possibility is ruled out by our dimuon measurements as shown in Figure 5.

This research was funded by the United States Department of Energy and the National Science Foundation.

References

1. W.K.Sakumoto *et al.*, *Nucl.Inst.Meth.*, **A294**, (1990) 179.
2. B.J.King *et al.*, *Nucl.Inst.Meth.*, **A302**, (1991) 254.
3. P.Auchincloss *et al.*, *Z.Phys.* **C48**, (1990) 411.
4. S.Dasu *et al.*, *Phys. Rev. Lett.* **61**, (1988) 1061.
5. S.A. Rabinowitz *et al.*, *Phys. Rev. Lett.* **70** (1993) 134.
6. A.De Rùjula *et al.*, *Nucl. Phys.*, **B154**, (1979) 394.
7. S.R. Mishra *et. al.*, Preprint Nevis-1459 (1992), Submitted to *Phys. Lett.*;W.C. Leung *et. al.*, Preprint Nevis-1460 (1992), Submitted to *Phys.Lett.*; P.Z. Quintas *et. al.*, Preprint Nevis-1461 (1992), Submitted to *Phys. Rev. Lett.*;
8. D. Duke and J. Owens, *Phys. Rev.* **D30** (1984) 49.
9. P.H Sandler *et al.*, *Zeit. Phys.* **C57** (1993) 1.
10. M.A.G. Aivazis, F.I. Olness, and W.K. Tung, *Phys. Rev. Lett.* **65** (1990) 2339
11. L.Whitlow, Ph.D. Thesis, SLAC - Report - 357 (1990) .
12. P. Amaudruz *et al.*, *Phys. Lett.* **B295** (1992) 159
13. A.C.Benvenuti *et al.*, *Phys. Lett.* **B223**, (1989) 485; **B237**, (1990) 592..
14. A.Bodek *et al.*, *Phys. Rev. Lett.* 50 (1983) 1431; 51 (1983) 534.
15. J. Botts *et al.*, Preprint Fermilab-Pub-92/371, Submitted to *Phys. Lett.*.

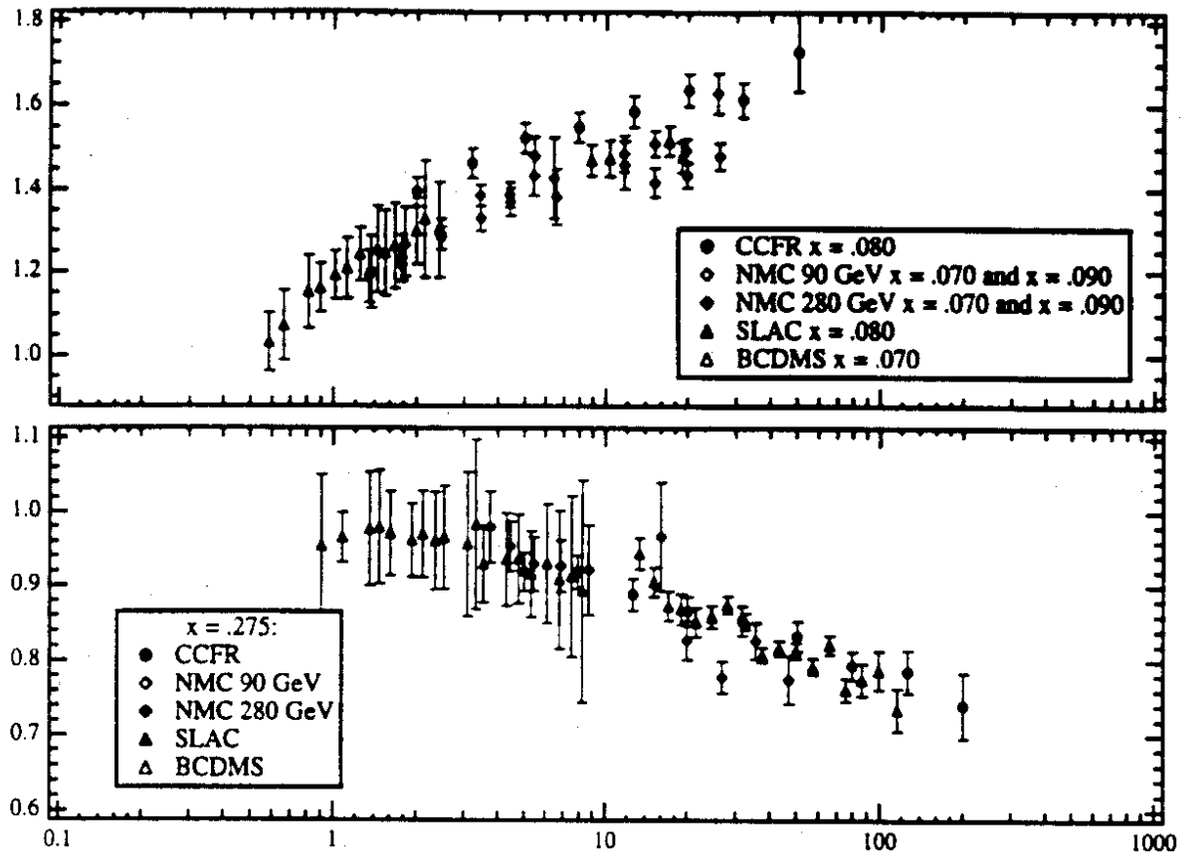

Figure 4: Comparison of the F_2 values measured by CCFR (νFe), SLAC (eD), NMC (μD), and BCDMS (μD) for $x = .080$ and .275. The lepton-deuterium results have been converted to be equivalent to νFe scattering using the " 5/18ths rule "with the strange sea extracted from our dimuon data and the heavy target correction.

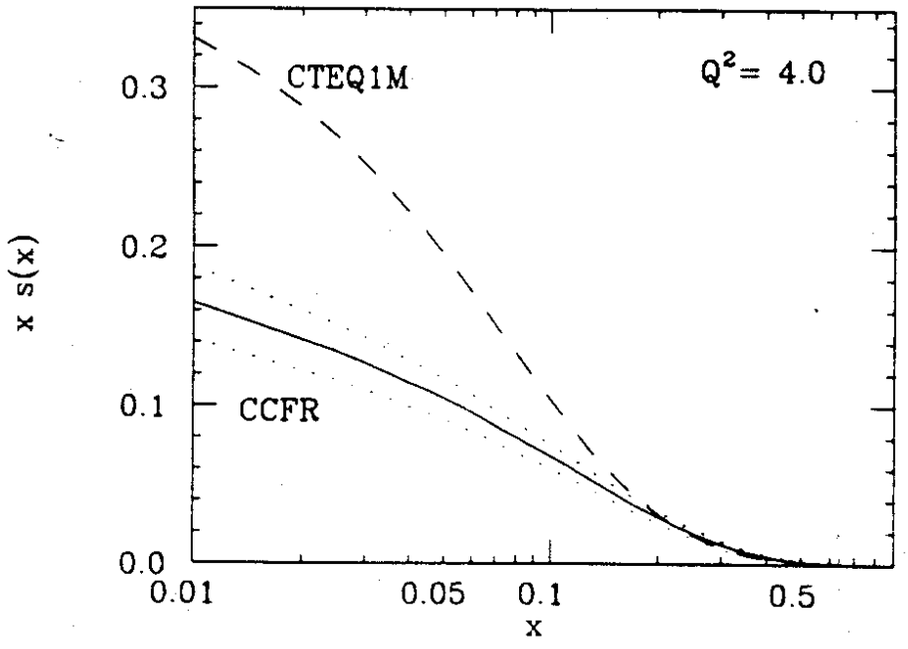

Figure 5: The strange-sea x distribution extracted from the CCFR dimuon data compared to the distribution of the CTEQ global fit. The band on the CCFR curve indicates the 1σ uncertainty in the distribution.